PHYSICAL REVIEW B VOLUME 21, NUMBER 4 15 FEBRUARY 1980

Electronic states in thorium under pressure

H. L. Skriver
Risø National Laboratory, DK-4000 Roskilde, Denmark

J.-P. Jan
National Research Council of Canada, Division of Physics, Ottawa K1A OR6, Canada
(Received 15 May 1979)

We have used the local-density formalism and the atomic-sphere approximation to calculate self-consistently the electronic properties of thorium at pressures up to 400 kbar. The derived equation of state agrees very well with static pressure experiments and shock data. Below the Fermi level (E_F) the electronic band structure is formed by 7*s* and 6*d* states while the bottom of a relatively broad 5*f* band is positioned 0.07 Ry above E_F. The calculated extremal areas of the Fermi surface and their calculated pressure dependence agree with earlier calculations and with de Haas–van Alphen measurements supporting the validity of the itinerant description of the 5*f* electrons for the light actinides. The calculation shows that the gradual *s* to *d* transition taking place at pressures up to 200 kbar is the cause of the unusual pressure dependence of the Fermi surface seen experimentally.

I. INTRODUCTION

Among the actinides, thorium plays, in some respect, a role similar to that of copper among the transition metals. It is relatively abundant, it has a simple crystal structure (fcc below 1400 °C), and it was the first element in its series for which its Fermi surface was obtained experimentally[1,2] as well as theoretically.[3-5] Since thorium is at the beginning of the actinide series it has unoccupied 5*f* transitional states close to the Fermi level. One may therefore expect its Fermi surface to be simple, and observably but only weakly affected by the presence of the 5*f* states. For this reason thorium has to some extent served as a test case for band calculations in the 5*f* transition series.

The Fermi surface found in the pioneering work by Loucks and co-workers[3-5] is indeed simple, consisting of only three closed pieces. Furthermore, these authors found that they could account qualitatively for the Fermi surface found in the de Haas–van Alphen experiments if they artificially removed the 5*f* bands. Later refinements by Koelling and Freeman[6,7] showed, however, that the inclusion of these 5*f* states in the band picture gave improved quantitative agreement with the measured Fermi surface. This was taken as evidence for the itinerancy of the 5*f* electrons at least in the lighter actinides, a claim that has been substantiated by other band calculations,[8,9] by careful examination of cohesive energies,[10] and most recently by calculations of the atomic volume through most of the actinide series.[11]

All of the previous band calculations are non-self-consistent and have used the Slater $X\alpha$ exchange-correlation potential[12] with α varying from 1 to $\frac{2}{3}$. It is the purpose of the present paper to employ the conceptually more satisfactory scheme of Hohenberg and Kohn[13] and Kohn and Sham[14] for ground-state properties in order to calculate and understand the electronic structure of thorium under pressure. Similar calculations have previously been performed on palladium[15] with considerable success, and most recently Glötzel[16] used essentially the present scheme to account for several ground state properties of thorium, cerium, and lanthanum.

Recent de Haas–van Alphen measurements by Schirber *et al.*[17] show that all of the observed orbits decrease in size with increasing pressure, contrary to the predictions of simple energy-band scaling models. The same authors attempted an explanation in terms of non-self-consistent band calculations, and they concluded that self-consistency was needed in order to understand their unexpected experimental results in details. In the present paper we present such self-consistent energy-band calculations, which do indeed offer an explanation of the Fermi surface data for thorium at low pressures. In addition we show that the same one-electron procedure, within the limitations of the so-called frozen-core approximation, can explain the electronic structure of thorium also at high pressures.

II. ONE-ELECTRON THEORY

The present technique is based on the local-density approximation to the density-functional formalism of Hohenberg and Kohn[13] and Kohn and Sham,[14] and we use the exchange-correlation potential devised by Barth and Hedin.[18] The original complicated many-body problem is thus reduced

to a one-electron description, but one still has to perform self-consistent energy-band calculations. To do this, we take advantage of the atomic-sphere approximation (ASA) to the linear-muffin-tin-orbitals (LMTO) method[19] of Andersen which gives rise to an extremely efficient self-consistency procedure.

There are two basic ingredients in this approach to band theory. First, the use of energy-independent muffin-tin orbitals leads to linear energy band methods, such as the LMTO method, which are orders of magnitude faster than the methods commonly used. Second, the atomic sphere approximation gives rise to the concept of canonical bands and the scaling technique which transforms these into unhybridized energy bands. When combined, these two features form the basis of our self-consistency procedure, which was developed by Andersen and co-workers[20-23] for use in calculations of ground state properties of transition metals.

In order to illustrate the techniques[24] involved let us consider the density of conduction electrons, spherically averaged over the atomic sphere of radius S as obtained in the ASA

$$\rho(r) = (4\pi)^{-1} 2 \sum_l \int^{E_F} \phi_l^2(E, r)\, N_l(E)\, dE\,, \tag{1}$$

where $\phi_l(E, r)$ is the solution inside the atomic sphere of the radial Schrödinger equation and $N_l(E)$ is the l-projected state density. Since $N_l(E)$ is easily obtained in a LMTO band calculation one might proceed by calculating the electrostatic and exchange-correlation potential and solving for a new band structure and corresponding projected state density. However, at this stage it is more efficient to use the following result from canonical band theory:

$$2N_l(E) = \dot{P}_l(E) \left(\frac{\partial n(\vec{\mathrm{P}})}{\partial P_l} \right)_{\vec{\mathrm{P}}(E)}, \tag{2}$$

where $n(\vec{\mathrm{P}})$ is the canonical number-of-states function and the dot denotes differentiation with respect to energy. The potential function vector $\vec{\mathrm{P}}$ is defined through

$$\vec{\mathrm{P}} \equiv (P_s, P_p, P_d, \ldots), \tag{3}$$

$$P_l(E) = 2(2l+1)\,[D_l(E) + l + 1]/[D_l(E) - l]\,, \tag{4}$$

$$D_l(E) = S\,\phi_l'(E, S)/\phi_l(E, S)\,. \tag{5}$$

Since a given crystal potential $V^*(r)$ specifies a unique path $\vec{\mathrm{P}}^*(E)$ in P space, one may map out $n(\vec{\mathrm{P}})$ by performing band calculations for many different potentials. This tedious procedure may be circumvented by neglecting differential hybridization because, in that case, $\partial n/\partial P$ is linear in the sense that

$$\frac{\partial n(\vec{\mathrm{P}})}{\partial P_d} = \frac{\partial}{\partial P_d}\, n\{P_s[E_d^*(P_d)], P_p[E_d^*(P_d)], P_d, P_f[E_d^*(P_d)]\}\,, \tag{6}$$

and similarly for s, p, and f. Here E_d^* is the function inverse to $P_d^*(E)$.

In the neglected differential hybridization approximation, Eq. (2) reduces to a scaling of the individual projected state densities, and the self-consistency loop then consists of one band calculation and repeated use of Eqs. (1) and (2). When wave functions, potential functions, etc., are written in terms of potential parameters, this scheme involves only the solution of Poisson's equation and of the radial Schrödinger equation at three different energies. Even in the cases where differential hybridization cannot be neglected, the scaling procedure allows us to obtain a self-consistent solution without performing more than a few band calculations.

The above technique is used only for the conduction electrons, while core states are included in the frozen-core approximation. A core charge density is constructed by performing a self-consistent relativistic atomic calculation for the appropriate electronic configuration, and renormalizing the atomic charge density to the atomic sphere. In the present case we have frozen the entire radonlike core and thus neglected the effect of the relatively extended $6p$ states which may be regarded as the major source of error in our calculation. On the other hand, this type of frozen core approximation has worked extremely well for transition metals,[22,25] light rare earths (La, Ce) and, most importantly, for all the light actinides[11] (Ra–Cm). In the ASA the electronic pressure may be calculated from the relations

$$3PV = \sum_l \int^{E_F} dE\, N_l(E)\, S\phi_l^2(E, S)\, \frac{-\delta D_l(E)}{\delta \ln S}\,,$$

$$-\frac{\delta D_l(E)}{\delta \ln S} = (D_l(E) + l + 1)(D_l(E) - l) + (E - \epsilon_{xc})\,S\,, \tag{7}$$

where ϵ_{xc} is the exchange-correlation energy taken at the atomic radius. These expressions are only slightly more complicated than Eq. (1), and imply that one may separate the total pressure into individual s, p, d, and f contributions. It is precisely because of this separation, which is inherent in the ASA, and which also applies to other quantities, that the ASA is so useful for the understanding of trends and variations among the elements.

III. EQUATION OF STATE

The high-pressure electronic properties of thorium as obtained by means of the local density and the atomic sphere approximations are presented in Fig. 1. At pressures below 100 kbar the calculated equation of state, Fig. 1(a), shows extremely good agreement with static pressure measurements.[26] Strictly speaking the theory is only valid at 0 K while the measurements were made at room temperature. However, both theory and experiment are normalized by the equilibrium atomic volume and the difference in temperature is therefore insignificant. At pressures above 200 kbar we compare with shock data.[27] Since these data contain an increasing pressure contribution with decreasing volume from the heating of the sample, the agreement with theory may also be considered as satisfactory in this pressure range. As a final point, one may note that the theoretical equation of state provides an accurate interpolation between the two sets of data, which is especially satisfying in view of the fact that the only input to the calculation is the atomic number of thorium.

The individual s, p, d, and f contributions to the pressure are presented in Fig. 1(b). As seen from the figure, the d pressure is negative and the d states provide at normal volume the main contribution to the metallic binding, while the s and p electrons are repulsive. In addition there is a negative f contribution to the pressure. This does not mean, however, that $5f$ orbitals are significantly occupied in thorium but rather that in the partial wave analysis, the tails of the s, p, and d waves give rise to an f contribution.

This question is clarified in Fig. 1(c), where we have plotted several band energies as function of the atomic radius. This shows that the $5f$ band is positioned above the Fermi level at low pressure and that it approaches E_F at increasing pressure and may eventually be occupied. It further shows that the p band is also well above E_F, and accordingly the only occupied states are those of the $6d$ and $7s$ bands. Finally, we note that the center of the s band moves through the Fermi level and that the p band moves steeply away from E_F.

TABLE I. Band masses μ_l and relative band-center positions $S^2C_{ls}=S^2(C_l-C_s)$ for thorium compared to free-electron values.

	S (a.u.)	3.4	3.756	3.9	Free electron
μ_l	s	0.58	0.63	0.66	1
	p	0.67	0.68	0.69	1
	d	1.57	1.88	2.03	1
	f	8.09	12.12	14.62	1
S^2C_{ls}	p	14.22	12.90	12.43	7.4
	d	3.01	4.35	4.68	17.7
	f	3.95	5.11	5.26	30.7

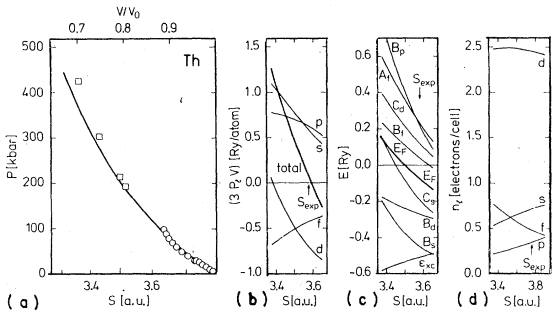

FIG. 1. Thorium under high pressure. (a) Calculated equation of state, solid line, compared to static pressure measurements (Ref. 26), open circles, and shock data (Ref. 27), open squares. (b) Partial pressures $3P_lV$ as a function of atomic radius. (c) Band energies, i.e., bottom of the l band B_l, center of the l band C_l, top of the l band A_l, Fermi energy E_F, and exchange-correlation energy ϵ_{xc} as function of atomic radius. The zero of energy is the electrostatic potential energy at the atomic sphere. (d) Number of l electrons at the Fermi level as a function of atomic radius.

The potential parameters listed in Table I show that the relative band-center energies C_{ds} and C_{fs} vary little with volume, while the variation in the bandwidth proportional to $(\mu_l S^2)^{-1}$ depends strongly on l. Table I further shows that the d and f electrons are far from being free-electron-like. All the above-mentioned movements of band energies are clearly reflected in Fig. 1(d), which shows that, as a function of decreasing volume, the number of s and p electrons decrease while the number of f electrons increases and n_d goes through a broad maximum at $S=3.5$ a.u. corresponding to a pressure of approximately 200 kbar. Thus, since the p and f states are unoccupied, an s to d transition is occurring, in which s electrons are being transferred to the d band under pressure.

IV. GROUND-STATE PROPERTIES

A few selected ground-state properties have been calculated, and they are compared to experiment[26,28-30] in Table II. The agreement we obtain is similar to that found in the transition metals, i.e., a few percent deviation for the equilibrium radius and a few-tens percent deviation for the bulk modulus. The calculation by Glötzel[16] is similar to ours except that he relaxed the outermost core p states which leads to a rather small equilibrium radius. The poor agreement with the dB/dP estimated from the static pressure data of Bridgman[26] is not surprising since this corresponds to the second de-

TABLE II. Calculated equilibrium atomic radius S, bulk modulus B, and the pressure derivative of B compared with experiment.

	Expt.	Theor.	
S (a.u.)	3.756[a]	3.787[e]	3.64[f]
B (kbar)	543[b], 580[c], 610[d]	632[e]	500[f]
dP/dB	6.6[b]	2.5[e]	3.4[f]

[a] Reference 28.
[b] Estimated from Ref. 26.
[c] Reference 29.
[d] Reference 30.
[e] Present results. B evaluated at calculated atomic radius.
[f] Reference 16. B evaluated at observed atomic radius.

rivative of the equation of state, and is therefore poorly determined, both experimentally and theoretically.

V. ENERGY BANDS

The calculated self-consistent relativistic band structure for thorium at the observed equilibrium volume is presented in Fig. 2. In the range below the Fermi level our bands are similar to those of Gupta and Loucks[4,5] who used full $X\alpha$ exchange[12] and artifically removed the $5f$ bands. In addition, we find close agreement with the bands of Freeman and Koelling[9] who used $\frac{2}{3}$ exchange and included the $5f$ states.

Within the atomic-sphere approximation, it is possible to obtain an approximate decomposition of a band structure by comparing unhybridized energy bands with fully hybridized bands. In Fig. 3 we show such a comparison, and the overall picture one obtains is that, below the Fermi level, the band structure is dominated by the s and d states while a relatively narrow f band (width of the order of 0.25 Ry) is positioned with its bottom 0.07 Ry ($\Gamma_2' - E_F$) above E_F. One may, furthermore infer that the fd hybridization will only slightly modify the shape of the Fermi surface, which is otherwise determined by the sd states and their hybridization. Finally, by comparing Fig. 3(a) with Fig. 2, one may judge the effect of spin-orbit coupling, which is seen to be important for the topology of the Fermi surface.

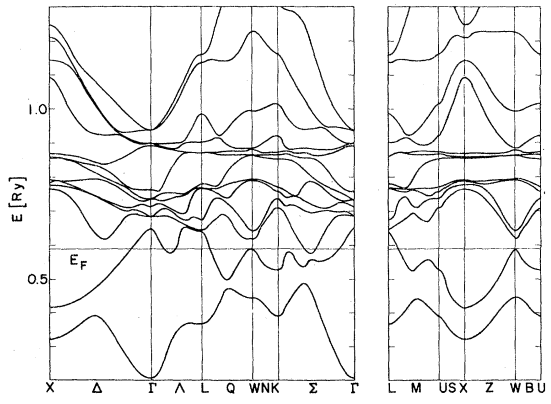

FIG. 2. Self-consistent relativistic energy bands for thorium at the observed equilibrium radius $S = 3.756$ a.u. The calculation includes spin-orbit coupling and the correction to the atomic-sphere approximation (Ref. 19). The zero of energy is taken to be the potential energy at the atomic sphere, which is essentially the muffin-tin zero.

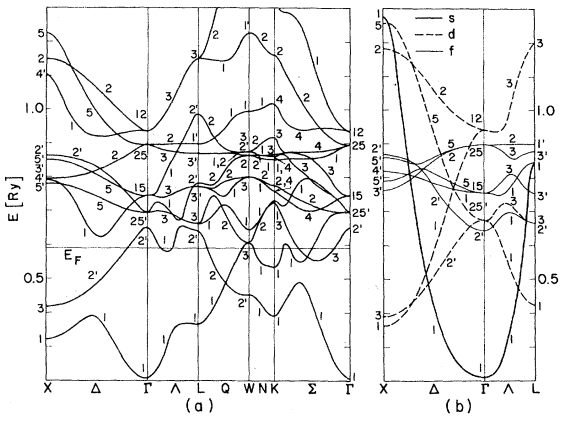

FIG. 3. Self-consistent relativistic energy bands for thorium. (a) Bands calculated without the spin-orbit interaction but with the correction to the ASA included. (b) Unhybridized s, d, and f bands.

The projected state densities[31] shown in Fig. 4 represent a decomposition which is less approximate than the unhybridized bands. It is clearly seen in Fig. 4 that, although the d character dominates below E_F, there is still appreciable f character through hybridization. Thus at the Fermi level the f states contribute 30% of the total state density. From the band structure of Fig. 2 we calculate the density of states at the Fermi level to be 15.0 [states/atom Ry] which may be compared to the measured[32] electronic specific-heat coefficient of 4.31 [mJ/mol K] corresponding to 24.8 states/atom Ry, giving an enchangement factor of 1.65. The electronic Grüneisen parameter $\frac{1}{3} d \ln N(E_F)/d \ln S$ is calculated to be 2.2. This is somewhat larger than the value $\frac{5}{3}$ expected for pure d bands, and indicates the importance of the sd and fd hybridization at the Fermi level.

VI. FERMI SURFACE

The theoretical Fermi surface of thorium was first established by Gupta and Loucks.[4,5] Their

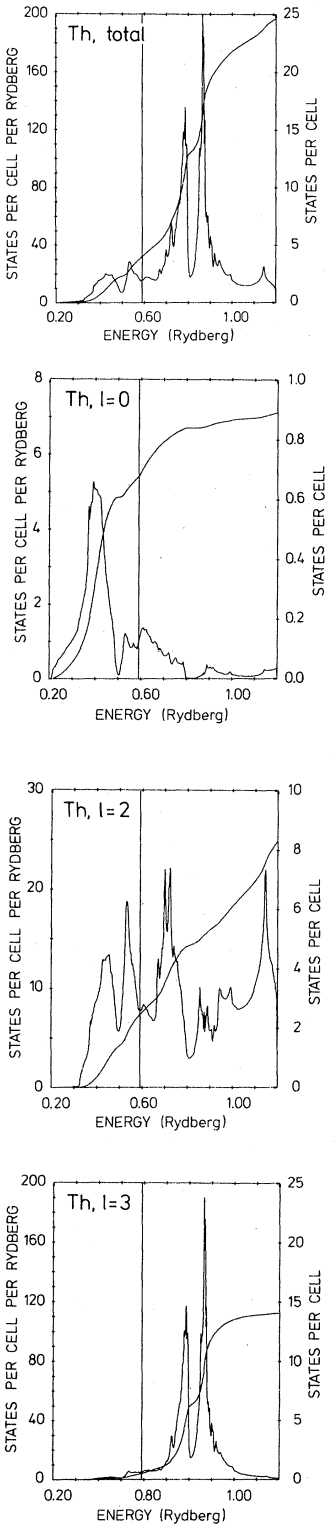

FIG. 4. Total and decomposed state densities for thorium. The calculation is without spin-orbit coupling but with the correction to the ASA, and corresponds to the bands of Fig. 3(a).

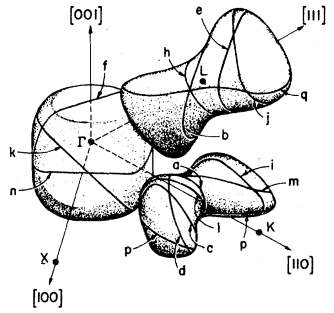

FIG. 5. Gupta-Loucks model of the Fermi surface for thorium [after Boyle and Gold (Ref. 2) as modified by Koelling and Freeman (Ref. 7)]. The extremal orbits indicated correspond to those listed in Tables III and IV.

model is shown in Fig. 5, and it consists of three closed pieces: (i) a hole surface centered at Γ (the "cube"), (ii) hole surfaces centered at L (the "dumbbells"), and (iii) compensating electron sheets on the symmetry line Σ (the "lungs"). Comparison with the de Haas–van Alphen experiments[2] showed that the topology of the calculated Fermi surface was correct and that the size of the lungs was in reasonable quantitative agreement with the measurements, while the cube was too large and the dumbbell too small.

Subsequent calculations,[7,9] which included the 5*f* states and used reduced exchange, confirmed the Gupta-Loucks interpretation of the de Haas–van Alphen measurements and showed quantitative agreement with the Fermi surface areas observed experimentally. The present calculation[33] also gives quantitative agreement with observation, as may be seen from Table III, where we list experimental and theoretical cross sections of the Fermi surface. The maximum shift in the Fermi level required to give complete agreement is 2 mRy for the cube, −14 mRy for the dumbbell, and −6 mRy for the lung. In agreement with Koelling and Freeman[7] we take this as evidence for the importance of hybridization with the 5*f* electrons in thorium.

VII. PRESSURE DEPENDENCE OF THE FERMI SURFACE

In order to obtain further evidence for the itinerancy of the 5*f* electrons, Schirber *et al.*[17] performed de Haas–van Alphen measurements on thorium under pressure. They discovered that all the Fermi surface areas observed decreased with increasing pressure, in contrast to a simple scaling model. The same authors calculated the area of several Fermi surface orbits and found that most but not all areas decreased with decreasing

TABLE III. Experimental and calculated Fermi surface data for thorium.

Surface	Direction	Orbit	Extremal areas (a.u.) Expt.[a]	Calc.[c]	Calc.[d]	Calc.[a]	Effective mass Expt.[b]	Calc.[d]	Calc.[c]
Cube	001	N	0.0591	0.0612	0.0577	0.0564	0.75 ± 0.03	−0.55	−0.62
	110	F	0.0660	0.0711	0.0646	0.0628		−0.72	−0.88
	111	K	0.0674	0.0703	0.0651	0.0634		−0.69	−0.85
Dumbbell									
	001	Q		0.0429	0.0584			−0.81	−0.52
	110	B	0.0361	0.0262	0.0332	0.0321		−0.37	−0.25
	110	E	0.0529	0.0416	0.0499	0.0489		−0.41	−0.34
	111	H	0.0291	0.0210	0.0256	0.0249		−0.27	−0.19
	111	J	0.0599	0.0447	0.0584	0.0572		−0.48	−0.41
Lung	100	L	0.0267	0.0238	0.0265	0.0267	0.66 ± 0.03	0.55	0.38
	100	M	0.0315[b]	0.0284	0.0300		0.58 ± 0.03	0.34	0.35
	001	P		0.0574	0.0584			0.71	0.63
	$1\bar{1}0$	A	0.0054	0.0046	0.0042	0.0047		0.20	0.15
	$1\bar{1}0$	C	0.0425	0.0322	0.0364	0.0382		0.67	0.60
	011	D	0.0257	0.0229	0.0222	0.0233	0.58 ± 0.01	0.44	0.32

[a] Reference 17. Note that the orbits C and D have been interchanged in order to be consistent with Ref. 7 and our Fig. 5.
[b] Reference 2 as quoted by Ref. 7.
[c] Present results.
[d] Reference 7.

atomic volume, and they attributed this unexpected volume dependence to the sd hybridization.

We have calculated[33] the volume derivative $d\ln A/d\ln\Omega$ of the Fermi surface cross sections in thorium and show the results in Table IV. The agreement with experiments is excellent and confirms the observation that most of the areas, but not all, decrease with increasing pressure.

In order to understand this situation let us consider the following expression[15] for the volume derivative of a Fermi surface area in a pure l band:

$$\frac{d\ln A_l}{d\ln\Omega} = -\frac{2}{3} + \frac{(E_F - C_l)\,\pi m_l^*}{3A_l}\left(\frac{d\ln(E_F - C_l)}{d\ln S} + \alpha_l\right), \qquad (8)$$

$$\alpha_l = \frac{d\ln(\mu_l S^2)}{d\ln S},$$

where m_l^* is the effective mass of the orbit in question. Since the bandwidth varies as $(\mu S^2)^{-1}$ the terms in the parentheses represent the rate by which the movement of the Fermi level is out of step with the band broadening. If we have only pure l bands, $E_F - C_l$ varies as $S^{-\alpha}$ and the volume derivative $d\ln A/d\ln\Omega$ is $-\frac{2}{3}$. Thus, for the pressure derivative $d\ln A/dp$, a value of $\frac{2}{3}B^{-1}$ signifies a "pure" behavior.

In the present case where s electrons are being exchanged for d electrons, α_d is 4.12 and we calculate $d\ln(E_F - C_d)/d\ln S$ to be −2.51, which is far from the pure value −5. Using typical values from Table III we find the volume derivative for d hole orbits to be 2.6. The agreement with the $d\ln A/d\ln\Omega$ values for the cube and the dumbbell (Table IV) shows that these hole sheets determine the position of the Fermi level. On the other hand, thorium is a compensated metal and the volume derivatives for the orbits on the electron lungs should therefore, in general, have the same sign as those of the hole orbits. The magnitude however, need not be so large since there are 12 lungs to compensate one cube and four dumbbells. Thus,

TABLE IV. Volume and pressure derivatives of Fermi surface areas for thorium.

			$\frac{d\ln A}{d\ln\Omega}$ Calc.	$\frac{d\ln F}{dP}$ Calc.[a]	(10^{-4} kbar^{-1}) Expt.[b]
Cube	001	N	2.29	−39	−38, −40
	110	F	2.45	−42	−38
	111	K	2.33	−40	
Dumbbell					
	001	Q	2.74	−47	
	110	B	1.96	−34	
	110	E	0.18	−3	−12, −11, −13
	111	H	1.97	−34	−39
	111	J	~0		
Lung	100	L	0.68	−12	−4.4
	100	M	0.57	−10	
	001	P	~0	~0	
	$1\bar{1}0$	A	0.93	−16	−50, −60
	$1\bar{1}0$	C	0.31	−5	
	001	D	0.33	−6	−3.4

[a] Obtained by multiplying $d\ln A/d\ln\Omega$ by the experimental $d\ln\Omega/dp = -1/B = -1.72\times10^{-3}$ kbar^{-1} (Ref. 29).
[b] Reference 17.

the s-to-d transition which takes place in thorium under increasing pressure and the compensation which must occur is responsible for the somewhat unexpected pressure derivative of the areas of the Fermi surface.

VII. CONCLUSION

We have performed self-consistent energy-band calculations for thorium at pressures up to 400 kbar by means of the local density formalism in conjunction with the atomic sphere approximation. Below the Fermi level the band structure is formed by the $7s$ and $6d$ states while a $5f$ band is positioned above the Fermi level, but hybridizes with the sd bands below E_F. The derived equation of state describes the static pressure and the shock data extremely well, and the results show that at pressures up to 200 kbar, s electrons are being transferred into the d band. The calculated extremal areas of the Fermi surface as well as their calculated pressure dependence is found to be in good agreement with de Haas–van Alphen measurements. Furthermore, the comparison shows that the above-mentioned s-to-d transition is the cause of the unusual pressure dependence of the Fermi surface found experimentally in thorium. In summary, it has been possible within the local-density formalism to account for the electronic properties of thorium metal as they manifest themselves at low pressure in Fermi-surface data and at high pressure in shock data.

ACKNOWLEDGMENTS

It is a pleasure to acknowledge discussions with O. K. Andersen, B. Johansson, A. R. Mackintosh, and J. E. Schirber.

[1]A. C. Thorsen, A. S. Joseph, and L. E. Valby, Phys. Rev. 162, 574 (1967).
[2]D. J. Boyle and A. V. Gold, Phys. Rev. Lett. 22, 461 (1969).
[3]S. C. Keaton and Y. L. Loucks, Phys. Rev. 146, 429 (1966).
[4]R. P. Gupta and T. L. Loucks, Phys. Rev. Lett. 22, 458 (1969).
[5]R. P. Gupta and T. L. Loucks, Phys. Rev. B 3, 1834 (1971).
[6]D. D. Koelling and A. J. Freeman, Solid State Commun. 9, 1369 (1971).
[7]D. D. Koelling and A. J. Freeman, Phys. Rev. B 12, 5622 (1975).
[8]E. A. Kmetko and H. H. Hill, in *Plutonium* 70, edited by W. N. Miner (AIME, New York, 1970), p. 233.
[9]A. J. Freeman and D. D. Koelling, in *The Actinides: Electronic and Related Properties*, edited by A. J. Freeman and J. B. Darby (Academic, New York, 1974), Vol. I, p. 51.
[10]B. Johansson and A. Rosengren, Phys. Rev. B 11, 1367 (1975).
[11]H. L. Skriver, O. K. Andersen, and B. Johansson, Phys. Rev. Lett. 41, 42 (1978).
[12]See, for instance, J. C. Slater, *The Self-Consistent Field for Molecules and Solids* (McGraw-Hill, New York, 1974).
[13]P. Hohenberg and W. Kohn, Phys. Rev. 136, B864 (1964).
[14]W. Kohn and L. J. Sham, Phys. Rev. 140, A1133 (1965).
[15]H. L. Skriver, W. Venema, E. Walker, and R. Griessen, J. Phys. F 8, 2313 (1978).
[16]D. Glötzel, J. Phys. F 8, L163 (1978); 8, L205 (1978).
[17]J. E. Schirber, F. A. Schmidt, and D. D. Koelling, Phys. Rev. B 16, 4235 (1977).
[18]U. von Barth and L. Hedin, J. Phys. C 5, 1629 (1972).
[19]O. K. Andersen, Phys. Rev. B 12, 3060 (1975).
[20]O. Jepsen, in *Magnetism and Magnetic Materials–1975 (Philadelphia), Proceedings of the 21st Annual Conference on Magnetism and Magnetic Materials*, edited by J. J. Becker, G. H. Lander, and J. J. Rhyne (AIP, New York, 1976), p. 327.
[21]U. K. Poulsen, J. Kollar, and O. K. Andersen, J. Phys. F 6, 587 (1976).
[22]O. K. Andersen, J. Madsen, U. K. Poulsen, O. Jepsen, and J. Kollar, Physica (Utrecht) 86-88B, 249 (1977).
[23]O. K. Andersen and O. Jepsen, Physica (Utrecht) 91B, 317 (1977).
[24]For a complete description, see A. R. Mackintosh and O. K. Andersen in *Electrons at the Fermi Surface*, edited by M. Springford (Cambridge University Press, Cambridge, in press).
[25]Y. Glötzel, D. Glötzel, and O. K. Andersen (unpublished).
[26]P. W. Bridgman, Proc. Am. Acad. Arts Sci. 77, 189 (1949).
[27]J. M. Walsh, M. H. Rice, R. G. McQueen, and F. L. Yarger, Phys. Rev. 108, 196 (1957).
[28]W. B. Pearson *A Handbook of Lattice Spacings and Structures of Metal Alloys* (Pergamon, New York, 1964).
[29]P. E. Armstrong, O. N. Carlson, and J. F. Smith, J. Appl. Phys. 30, 36 (1959).
[30]M. B. Reynolds, U. S. Atomic Energy Commission Report No. AECD-3242, 1951 (unpublished).
[31]Projected state densities were calculated from LMTO eigenvalues and eigenvectors at 240 points in the irreducible zone using the tetrahedron method of O. Jepsen and O. K. Andersen [Solid State Commun. 9, 1763 (1971)]. The calculation does not include the spin-orbit interaction, but the correction to the ASA (Ref. 19) is taken into account.
[32]J. E. Gordon, H. Montgomery, R. J. Noer, G. R. Picket, and R. Torbon, Phys. Rev. 152, 432 (1966).
[33]The extremal areas corresponding to the bands of

Fig. 2 were calculated as follows. Cube and dumbbell: 61-star Fourier fit to the 240 first principles points in the irreducible zone, and orbit tracking. Lung: 61-star fit, interpolation over 916-point mesh and integration by the tetrahedron technique. The Fermi level was determined by tetrahedron integration over an interpolated 916-point mesh. Volume derivatives were obtained from band structures calculated at $s=3.7$, 3.75, 3.7557, and 3.8 a.u. All calculations were performed using the correction to the ASA (Ref. 19) and included spin-orbit interaction.